INTERNATIONAL JOURNAL OF IMMUNOPATHOLOGY AND PHARMACOLOGY Vol. 23, no. 4, 1033-1046 (2010)

GW0742, A HIGH AFFINITY PPAR-β/δ AGONIST REDUCES LUNG INFLAMMATION INDUCED BY BLEOMYCIN INSTILLATION IN MICE

M. GALUPPO[1], R. DI PAOLA[2], E. MAZZON[1], E. ESPOSITO[1], I. PATERNITI[2], A. KAPOOR[3], C. THIEMERMANN[3] and S. CUZZOCREA[1,2]

[1]Department of Clinical and Experimental Medicine and Pharmacology, School of Medicine, University of Messina, Italy; [2]IRCCS Centro Neurolesi "Bonino-Pulejo", Messina, Italy; [3]The William Harvey Research Institute, Centre for Experimental Medicine, Nephrology and Critical Care, St Bartholomew's and The Royal London School of Medicine and Dentistry, London, UK

Received January 15, 2010 – Accepted September 10, 2010

The first two authors contributed equally to this work

Peroxisome Proliferator-Activated Receptor β/δ belongs to a family of ligand-activated transcription factors. Recent data have clarified its metabolic roles and enhanced the potential role of this receptor as a pharmacological target. Moreover, although its role in acute inflammation remains unclear, being the nuclear receptor PPAR β/δ widely expressed in many tissues, including the vascular endothelium, we assume that the infiltration of PMNs into tissues, a prominent feature in inflammation, may also be related to PPAR β/δ. Mice subjected to intratracheal instillation of bleomycin (BLEO, 1 mg/kg), a glycopeptide produced by the bacterium Streptomyces verticillus, develop lung inflammation and injury characterized by a significant neutrophil infiltration and tissue oedema. Therefore, the aim of this study is to investigate the effects of GW0742, a synthetic high affinity PPAR β/δ agonist, and its possible role in preventing the advance of inflammatory and apoptotic processes induced by bleomycin, that long-term leads to the appearance of pulmonary fibrosis. Our data showed that GW0742-treatment (0.3 mg/Kg, 10% DMSO, i.p.) has therapeutic effects on pulmonary damage, decreasing many inflammatory and apoptotic parameters detected by measurement of: 1) cytokine production; 2) leukocyte accumulation, indirectly measured as decrease of myeloperoxidase (MPO) activity; 3) IκBα degradation and NF-κB nuclear translocation; 4) ERK phosphorylation; 5) stress oxidative by NO formation due to iNOS expression; 6) nitrotyrosine and PAR localization; 7) the degree of apoptosis, evaluated by Bax and Bcl-2 balance, FAS ligand expression and TUNEL staining. Taken together, our results clearly show that GW0742 reduces the lung injury and inflammation due to the intratracheal BLEO–instillation in mice.

Pulmonary fibrosis is a common response to various insults to the lung and it is the end-point of a numerous and heterogeneous group of disorders known as interstitial lung diseases (ILD), that are characterized by chronic inflammation and progressive fibrosis of the pulmonary interstitium; as a consequence, pathological changes occur in the alveolar walls (including epithelial cells, and capillaries), septae, and the perivascular,

Key words: inflammation, NFkB activation, macrophage inflammatory protein, cytokines

Mailing address: Salvatore Cuzzocrea, Ph. M.D.
Dip. Clinico e Sperimentale di Medicina e Farmacologia,
Torre Biologica,
Policlinico Universitario,
98123 Messina, Italy
Tel: ++39 090 2213644, Fax: ++39 0902213300,
e-mail: salvator@unime.it

0394-6320 (2010)

perilymphatic, and peribronchiolar connective tissues (1). Pathological findings in this disease include temporally and spatially non-homogeneous areas of inflammation and fibrosis. Microscopically, the hyperplasia of type II pneumocytes and active fibroblast proliferation leads to excessive matrix deposition resulting in the irreversible distortion of the lung architecture (2), which in turn is responsible for impaired gas exchanges and respiratory failure. A number of exogenously administered agents are known to induce an iatrogenic form of pulmonary fibrosis (3).

The Bleomycin (BLEO) instillation is the best characterized murine model in use today to induce lung injury and fibrosis in a wide variety of experimental animals (4). The studies looking at inflammation, cytokines, chemokines and growth factors as precursors of the bleomycin-induced fibrosis are numerous.

In this work, we consider that it is important to assess the advance of the inflammatory process and the following activation of apoptotic pathways in absence or presence of PPARβ/δ activation by GW0742-treatment, believing that the regulatory effects of this receptor might play an important role in controlling the phases leading to the appearance of pulmonary fibrosis.

We showed that PPARβ/δ has unexpected anti-inflammatory properties, comparable with evidence in the literature regarding the other members of the family of PPARs (5).

PPARs regulate gene expression by binding, as heterodimers, with retinoid X receptors (the 9-cis-retinoic acid receptors or RXRs) to specific PPAR response elements (PPRE) in the promoter regions of specific target genes. They play important roles in the regulation of metabolic pathways, as well as in a variety of cell differentiation, proliferation and apoptosis pathways (6-8). Recently studies have also shown a possible role of the PPARs in the regulation of inflammation and immune responses (9).

As opposed to PPARα and -γ, little is still known about the vascular role of PPAR β/δ (10). In this study, we found that, after bleomycin instillation, the treatment with GW0742, a synthetic high affinity PPARβ/δ ligand, significantly decreases the inflammatory processes in the lung and, in particular, 1) lung injury; 2) TNF-α and IL-1β levels; 3) oxidative stress; 4) the alteration of IκB-α/NF-κB balance; 5) MAP kinase signalling pathway and (6) apoptosis.

MATERIALS AND METHODS

Animals

Male CD mice (25-35 g; Harlan Nossan, Italy) were housed in a controlled environment and provided with standard rodent chow and water. Animal care was in compliance with Italian regulations on the protection of animals used for experimental and other scientific purposes (D.M. 116192) as well as with the EEC regulations (O.J. of E.C. L 358/1 12/18/1986).

Experimental groups

Mice were randomized into four experimental groups:

1. *Bleomycin-treated group*: mice were subjected to lung injury induced by intratracheal instillation of bleomycin and treated daily via intraperitoneal injection with vehicle of GW0742 (10% dimethylsulfoxide (DMSO, 1 ml/kg), 1 h after BLEO instillation (n=15).
2. *GW0742 group*: identical to Bleomycin-treated group but mice were treated daily with GW0742 (0.3 mg/kg, 1 h after BLEO instillation) via intraperitoneal injection (n=15).
3. *Sham-operated mice + vehicle group*: animals were subjected to the identical surgical procedure but received intra-tracheal instillation of saline (0.9%) instead of BLEO and were treated daily with the vehicle of GW0742 (10% dimethylsulfoxide (DMSO), 1 ml/kg, i.p.), 1 h after saline instillation (n=15).
4. *Sham-operated mice + GW0742 group*: identical to *sham + vehicle group* but mice were treated daily with GW0742 (0.3 mg/kg, 1 h after saline instillation) via intraperitoneal injection (n=15).

The mice were sacrificed after 7 days for analyses of injury, inflammation and apoptosis.

Induction of lung injury by bleomycin

Mice received a single intratracheal instillation of saline (0.9%) or saline containing bleomycin sulphate (1 mg/kg body weight) at end-expiration in a volume of 100 μl, and the liquid was followed immediately by 300 μl of air to ensure delivery to the distal airways and were sacrificed after 7 days by pentobarbitone overdose.

Measurement of fluid content in lung

Seven days after instillation of bleomycin, all mice

were sacrificed and a subset of these was used to measure the fluid content in the lung. Only one of the two lungs of animals belonging to each experimental group was used for this test, while the other was taken for biochemical assays. Briefly, by careful excision of the lung from other adjacent extraneous tissues, the tissue was weighed (wet weight), exposed for 48 h at 180°C and the dry weight was measured. Water content was calculated by subtracting dry weight from wet weight.

Histological examination

Lung biopsies were taken 7 days after injection of bleomycin. Lung biopsies were fixed for 1 week in 10% (w/v) PBS-buffered formaldehyde solution at room temperature, dehydrated using graded ethanol and embedded in Paraplast (Sherwood Medical, Mahwah, NJ, USA). After embedding in paraffin, the sections were prepared and stained by Masson's trichrome stain or hematoxylin and eosin, to identify inflammatory cells, connective tissue and fibrotic lesions. All sections were studied using light microscopy (Dialux 22 Leitz, Zeiss, Milan, Italy).

Terminal deoxynucleotidyl transferase-mediated dUTP-biotin end labelling assay

Terminal deoxynucleotidyl transferase-mediated dUTP-biotin end labelling assay (TUNEL) was conducted by using a TUNEL detection kit according to the manufacturer's instruction (Apotag horseradish peroxidase kit; DBA, Milan, Italy). Briefly, sections were incubated with 15.2 μg/mL proteinase K for 15 min at room temperature and then washed with PBS. Endogenous peroxidase was inactivated by 3% H_2O_2 for 5 min at room temperature and then washed with PBS. Sections were immersed in terminal deoxynucleotidyl transferase (TdT) buffer containing deoxynucleotidyl transferase and biotinylated deoxyuridine 5-triphosphate in TdT buffer, incubated in a humid atmosphere at 37°C for 90 min, and then washed with PBS. The sections were incubated at room temperature for 30 min with anti-fluorescein isothiocyanate horseradish peroxidase-conjugated antibody, and the signals were visualized with diaminobenzidine.

Immunohistochemical localization of TNF-α, IL-1β, iNOS, nitrotyrosine, PARP, Bax, Bcl-2 and FAS ligand

At the end of the experiment, the tissues were fixed in 10% (w/v) PBS-buffered formaldehyde and 8 μm sections were prepared from paraffin embedded tissues. After deparaffinization, endogenous peroxidase was quenched with 0.3% (v/v) hydrogen peroxide in 60% (v/v) methanol for 30 min. The sections were permeablized with 0.1% (w/v) Triton X-100 in PBS for 20 min. Non-specific adsorption was minimized by incubating the section in 2% (v/v) normal goat serum in PBS for 20 min. Endogenous biotin or avidin binding sites were blocked by sequential incubation for 15 min with biotin and avidin (DBA, Milan, Italy), respectively. Sections were incubated overnight with anti-TNF-α antibody (Santa Cruz Biotechnology, 1:500 in PBS, v/v), or with anti-IL-1β antibody (Santa Cruz Biotechnology, 1:500 in PBS, v/v), or with anti-iNOS antibody (Santa Cruz Biotechnology, 1:500 in PBS, v/v); or with anti-nitrotyrosine antibody (Upstate Biotech, 1:500 in PBS, v/v), or with anti-poly (ADP-ribose) antibody (Santa Cruz Biotechnology, 1:500 in PBS, v/v) or with anti-Bax antibody (Santa Cruz Biotechnology, 1:500 in PBS, v/v), or with anti-Bcl2 antibody (Santa Cruz Biotechnology, 1:500 in PBS, v/v) or with anti-FAS ligand antibody (Santa Cruz Biotechnology, 1:500 in PBS, v/v). Sections were washed with PBS, and incubated with secondary antibody. Specific labelling was detected with a biotin-conjugated goat anti-rabbit or anti-mouse IgG and avidin-biotin peroxidase complex (DBA, Milan, Italy).

Subcellular fractionation, nuclear protein extraction and Western blot analysis for iNOS, IkB-α, NF-κB p65, p-ERK, ERK2, Bax and Bcl-2

Tissues were homogenized in cold lysis buffer A (HEPES 10mM pH=7.9; KCl 10mM;EDTA 0.1mM; EGTA 0.1mM; DTT 1mM; PMSF 0.5mM; Trypsin inhibitor 15μg/ml; PepstatinA 3 μg/ml; Leupeptin 2 μg/ml; Benzamidine 40 μM). Homogenates were centrifuged at 12,000 g for 3 min at 4°C, and the supernatant (cytosol + membrane extract) was collected to evaluate contents of IkB-α, p-ERK, ERK2, Bax, Bcl-2 and β-actin. The pellet was resuspended in buffer C (HEPES 20mM; MgCl2 1.5 mM; NaCl 0.4mM; EDTA 1mM; EGTA 1mM; DTT 1mM; PMSF 0.5 μg/ml; Leupeptin 2 μg/ml; Benzamidine 40 μM; NONIDET P40 1%; Glycerol 20%) and centrifuged at 12,000 g for 12 min at 4°C, and the supernatant (nuclear extract) was collected to evaluate the content of NF-kB p65 and Lamin B1. Protein concentration in the homogenate was determined by Bio-Rad Protein Assay (BioRad, Richmond CA) and 50 μg of cytosol and nuclear extract from each sample was analysed. Proteins were separated by 12% SDS-polyacrylamide gel electrophoresis and transferred on to a PVDF membrane (Hybond-P Nitrocellulose, Amsherman Biosciences,UK). The membrane was blocked with 0.1% TBS-Tween containing 5% non-fat milk for 1 h at room temperature. After the blocking, the membranes were incubated with the relative primary antibody overnight at 4°C with anti-iNOS TYPE II (BD transduction laboratories, 1:1000) or anti-IkB-α (Santa Cruz Biotechnology, 1:1000) or anti-p-ERK (Santa Cruz Biotechnology, 1:500) or anti-ERK2 (Santa Cruz Biotechnology, 1:500) or anti-Bax

(Santa Cruz Biotechnology, 1:500) or anti-Bcl2 (Santa Cruz Biotechnology, 1:1000) or anti-β-actin (Sigma-Aldrich Corp 1:5000). The membranes with nuclear fractions were incubated with anti-NFkB p65 (Santa Cruz Biotechnology, 1:250) or anti-Lamin B1 (Sigma-Aldrich Corp., 1:10000).

After the incubation, the membranes were washed three times for ten minutes with 0.1% TBS Tween and were then incubated for one hour with peroxidase-conjugated anti-mouse or anti-rabbit secondary antibodies (Jackson ImmunoResearch Laboratories, USA, 1: 2000). The membranes were then washed three times for ten minutes and protein bands were detected with SuperSignal West Pico Chemioluminescent (PIERCE). Densitometry analysis was performed with a quantitative imaging system (ImageJ).

Myeloperoxidase activity

Myeloperoxidase (MPO) activity was determined as marker indirect of leukocyte accumulation. At the specified time following injection of bleomycin, lung tissues were obtained and weighed, each piece homogenised in a solution containing 0.5% (w/v) hexadecyltrimethyl-ammonium bromide dissolved in 10 mM potassium phosphate buffer (pH 7) and centrifuged for 30 min at 20,000 x g at 4°C. An aliquot of the supernatant was then allowed to react with a solution of tetramethylbenzidine (1.6 mM) and 0.1 mM hydrogen peroxide. The rate of change in absorbance was measured spectrophotometrically at 650 nm. MPO activity was defined as the quantity of enzyme degrading 1 μmol of peroxide/min at 37°C and was expressed in milliunits per g of wet tissue.

Measurement of cytokines

Portions of lung, collected at 7 days after bleomycin administration, were homogenized in PBS containing 2 mmol/L of phenyl-methyl sulfonyl fluoride (Sigma Chemical Co., Milan, Italy) and tissue levels of TNFα and IL-1β were evaluated. The assay was carried out by using a colorimetric, commercial kit (Calbiochem-Novabiochem Corporation, USA) according to the manufacturer's instructions. All cytokine determinations were performed in duplicate serial dilutions.

Materials

Unless otherwise stated, all compounds were obtained from Sigma-Aldrich Company Ltd. (Poole, Dorset, U.K.). All other chemicals were of the highest commercial grade available. All stock solutions were prepared in non-pyrogenic saline (0.9% NaCl; Baxter, Italy, UK).

Analysis

All values in the figures and text are expressed as mean ± standard error of the mean (SEM) of N observations. For the *in vivo* studies N represents the number of animals studied. In the experiments involving histology or immunohistochemistry, the figures shown are representative of at least three experiments (histological or immunohistochemistry coloration) performed on different experimental days on the tissues section collected from all the animals in each group. Data sets were examined by one- or two-way analysis of variance, and individual group means were then compared with Student's unpaired t-test. A P-value of less than 0.05 was considered significant.

RESULTS

Effects of GW0742 on BLEO-induced lung injury

Masson's trichrome stain of lung sections revealed significant tissue damage (Fig. 1C), when compared with sham-operated animals (Fig. 1A).

Seven days after bleomycin instillation, the pulmonary lesions observed in mice consisted of multifocal areas of severe inflammation (Fig. 1C). In these areas, an intense thickening of alveolar septa with evident infiltration of macrophages, lymphocytes, polymorphonuclear neutrophils and some eosinophils was observed. In contrast, 7 days after bleomycin instillation, a reduced intensity Masson-trichrome staining in GW0742-treated mice revealed that the PPARβ/δ agonist caused a less severe pattern of pulmonary lesion (Fig. 1E).

Moreover, histological examination, by Haematoxylin/Eosin staining, of lung sections taken from BLEO-instillated mice revealed significant tissue damage characterized by extensive inflammatory infiltration of neutrophils, lymphocytes and plasma cells (Fig. 1D), when compared to lung sections taken from sham-operated animals (Fig. 1B). Furthermore, BLEO-instillation elicited an acute inflammatory response characterized by the accumulation of fluid (oedema) in lung tissues (Fig. 1D). Administration of GW0742 significantly attenuated the histological signs of BLEO-induced lung injury, as well as oedema formation (Fig. 1F).

Effects of GW0742 on changes in body weight, fluid content and leukocyte accumulation in lung

The severe lung injury caused by BLEO-instillation was associated with a significant loss in body weight (Fig. 2A), while GW0742-treated mice

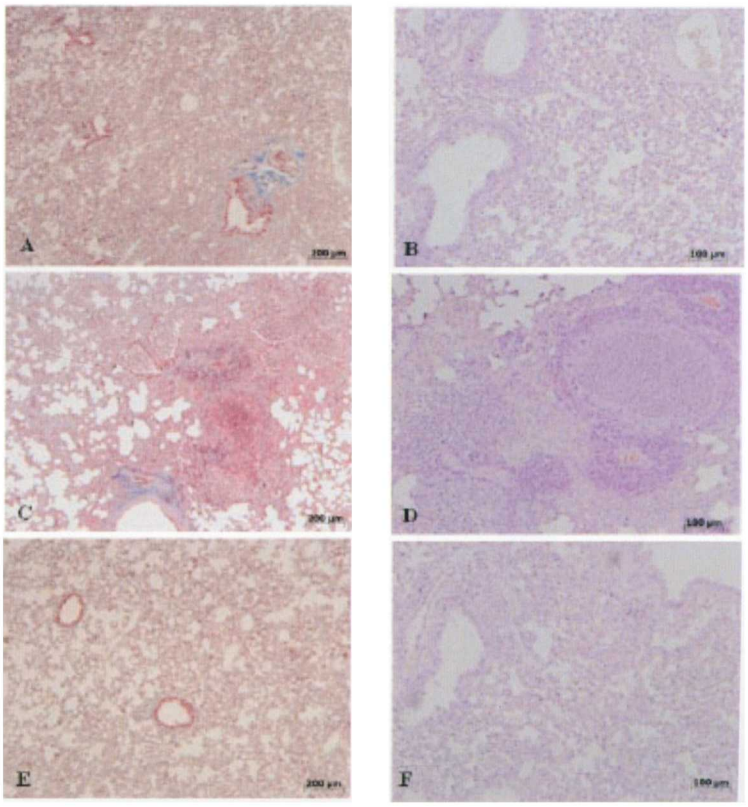

Fig. 1. *Masson's trichrome staining of lung sections revealed significant tissue damage (1C), when compared with sham-operated animals (1A). GW0742-treatment causes a decrease of pulmonary lesion (1E). Hematossilin/Eosin staining showed lung sections from sham-operated mice (1B) demonstrating the normal architecture of the lung. On the contrary, lung biopsies of bleomycin-instilled mice showed marked inflammatory changes (1D). GW0742-treatment significantly reduced the pathological changes in the tissues (1F). Figures are representative of at least 3 experiments performed on different experimental days.*

showed a reduction of the BLEO-induced loss body weight (Fig. 2A).

BLEO-instillation also caused an increase of wet/dry lung weight ratio, due to infiltration of inflammatory cells and oedema, when compared with sham-operated mice (Fig. 2B). On the contrary, GW0742-treated mice showed a significant decrease of wet/dry lung weight ratio (Fig. 2B). Moreover, this histological pattern of lung injury appeared to be correlated with an influx of leukocytes into the lung tissue. Therefore, we investigated the role of GW0742 on leukocyte infiltration by measurement of the activity of MPO. Myeloperoxidase levels were increased by BLEO-instillation, when compared with lung tissues obtained from sham-operated animals (Fig. 2C). In contrast, a decrease of MPO activity was observed in tissue sections taken from GW0742-treated mice after BLEO-instillation (Fig. 2C).

GW0742 modulates production and expression of TNF-α and IL-1β after BLEO-instillation

To test whether GW0742 may modulate the inflammatory process through regulation of the secretion of cytokines, we analyzed the lung levels of the pro-inflammatory cytokines TNF-α and IL-1β. A substantial increase in TNF-α and IL-1β formation was observed in lung samples taken 7 days after BLEO-instillation, when compared with sham-operated animals (Figs. 3Aa and Ab, respectively). In contrast, there was a significant inhibition of TNF-α and IL-1β in instilled-mice treated with GW0742 (Figs. 3Aa and Ab, respectively). In addition, tissue sections obtained from instilled mice demonstrate positive staining for TNF-α (Fig. 3Ba, see densitometry analysis Bh)

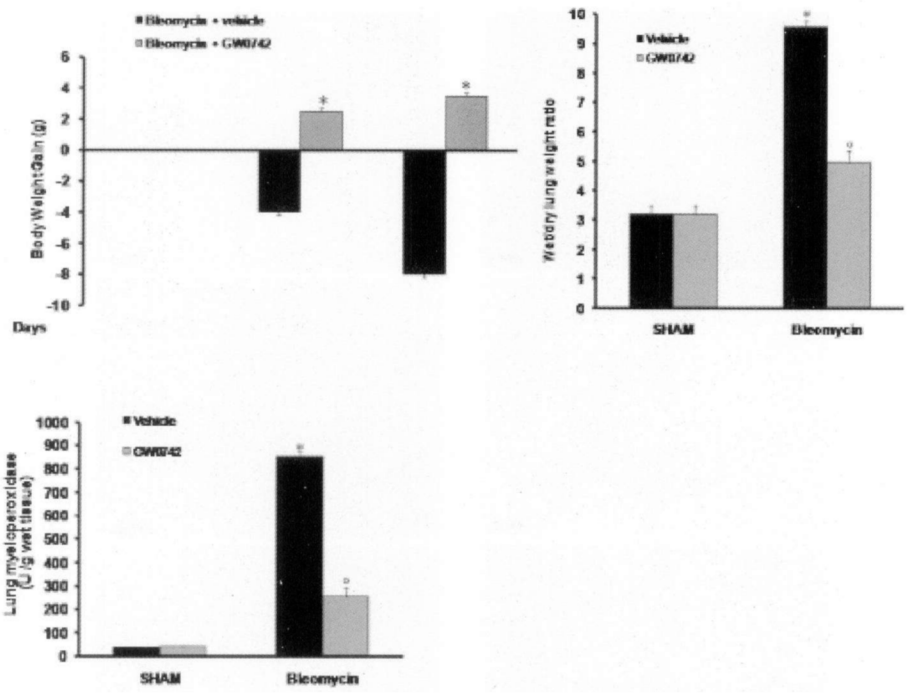

Fig. 2. *Bleomycin administration was associated with a significant loss in body weight, but GW0742-treatment significantly attenuated the loss (2A). BLEO also caused an increase of wet/dry lung weight ratio, due to infiltration of inflammatory cells and oedema, when compared with sham-operated animals. On the contrary, GW0742 showed a significant decrease of wet/dry lung weight ratio (2B). Moreover, myeloperoxidase levels were increased by BLEO-instillation, when compared to lung tissues obtained from sham-operated animals. In contrast, a decrease of MPO activity was observed in tissue sections taken from BLEO-instilled mice treated with GW0742 (2C). Data are mean ± standard deviation from n=10 mice for each group. *P<0.01 vs sham-operated mice, °P<0.01 vs bleomycin + vehicle.*

and IL-1β (Fig. 3Bb, see densitometry analysis Bh), mainly localized in the infiltrated inflammatory cells in damaged tissues. In GW0742-treated mice, the staining for TNF-α (Fig. 3Bc, see densitometry analysis Bh) and IL-1β (Fig. 3Bd, see densitometry analysis Bh) was visibly and significantly reduced when compared with BLEO-instilled mice treated with vehicle. In the lungs of sham-operated animals no positive staining was observed for TNF-α (data not shown) or IL-1β (data not shown).

Effect of GW0742 on IκB-α degradation and NF-κB p65 activation

To investigate the inflammatory cellular mechanisms by which treatment with GW0742 may attenuate the development of bleomycin-induced injury, we evaluated IκB-α degradation and nuclear NF-κB p65 translocation by Western blot analysis. A basal level of IκB-α was detected in the lung tissues of sham-operated animals (Fig. 4a, see densitometry analysis a1), whereas in BLEO-instilled mice, IκB-α levels were substantially reduced (Fig. 4a, see densitometry analysis a1). GW0742 prevented bleomycin-induced IκB-α degradation, with IκB-α levels observed in these animals similar to those of the sham-operated mice group (Fig. 4a, see densitometry analysis a1). In addition, BLEO-instillation caused a significant increase in NFkB p65 levels in the nuclear fractions from lung tissues, compared to the sham-operated mice (Fig. 4b, see densitometry analysis b1). GW0742-treatment significantly reduced the levels of NF-kB p65 in the lung (Fig. 4b, see densitometry analysis b1).

Effects of GW0742 on BLEO-induced iNOS expression nitrotyrosine formation and PARS activation

iNOS expression was assessed in samples of pulmonary tissue by Western blot analysis (Fig. 5Aa, see densitometry analysis Aa1). A significant increase in iNOS expression was demonstrated in samples of lung obtained from BLEO-instillated mice, when

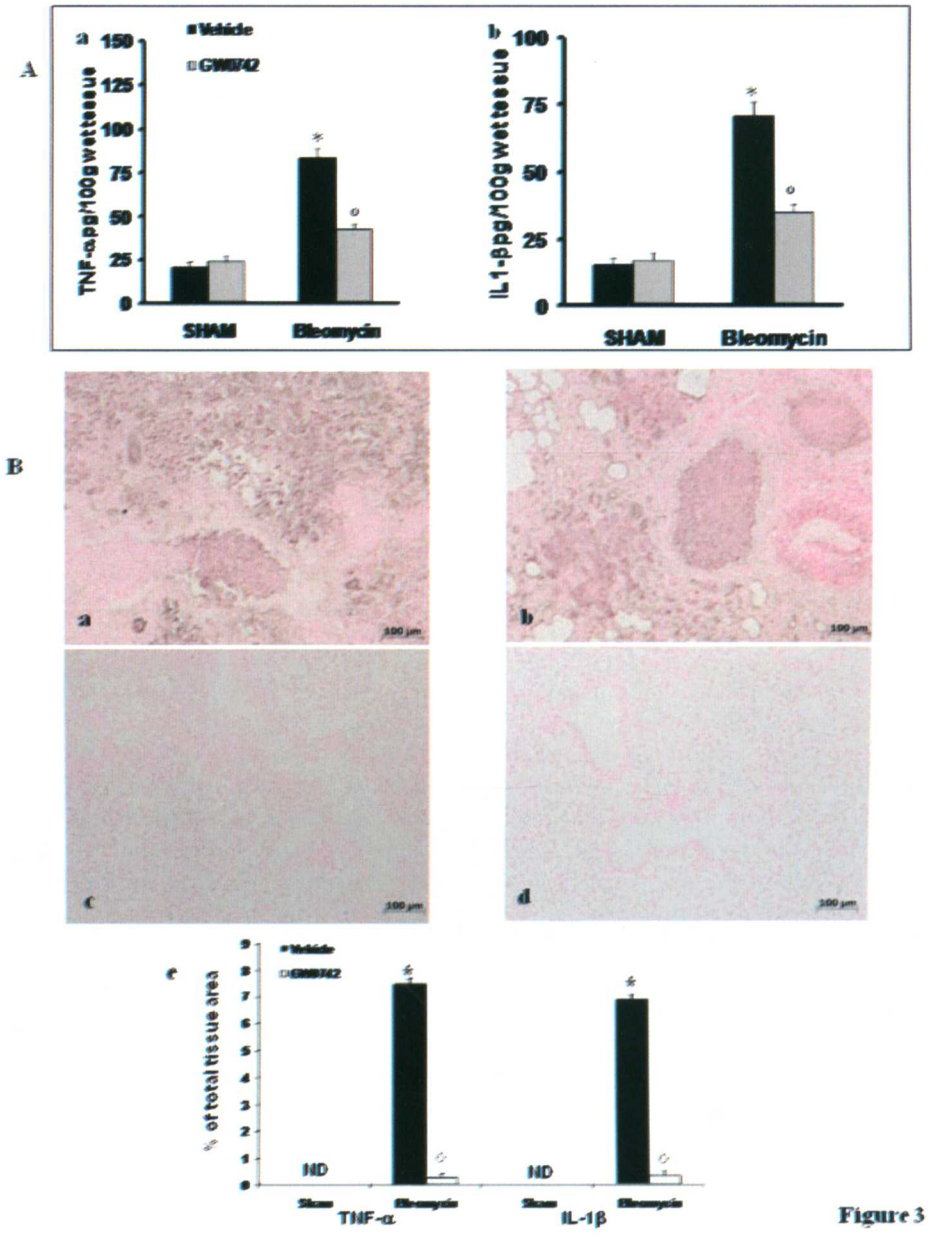

Fig. 3. *The evaluation of the pro-inflammatory cytokine lung production showed that in lung samples taken from mice 7 days after BLEO-instillation* there was a substantial increase in TNF-α (Aa) and IL-1β (Ab) formation when compared with *sham-operated animals (Aa and Ab, respectively). In contrast, in BLEO-instilled animals which were* treated with GW0742 there was a significant inhibition of TNF-α (Aa) and IL-1β and (Ab). Moreover, im*munohistochemical localization of proinflammatory cytokines in lung sections obtained from instilled mice* showed positive staining for TNF-α (Ba) and IL-1β (Bb), mainly localized in the infiltrated inflammatory cells in *damaged tissues. In GW0742-treated mice*, the staining for TNF-α (Bc) and IL-1β (Bd) was visibly and significantly reduced when compared with *instilled mice treated with vehicle. Densitometry analysis (e) of immunohistochemistry photographs (n=5 photos from* each sample collected from all mice in each experimental group) for TNF-α (Aa) and IL-1β was *assessed. The assay was carried out by using AxioVision on a personal computer. The figure is representative of at least three experiments performed on different experimental days. Data are expressed as % of total tissue area and are mean ± standard deviation from n=10 mice for each group. *P<0.01 vs sham-operated mice, °P<0.01 vs bleomycin + vehicle.*

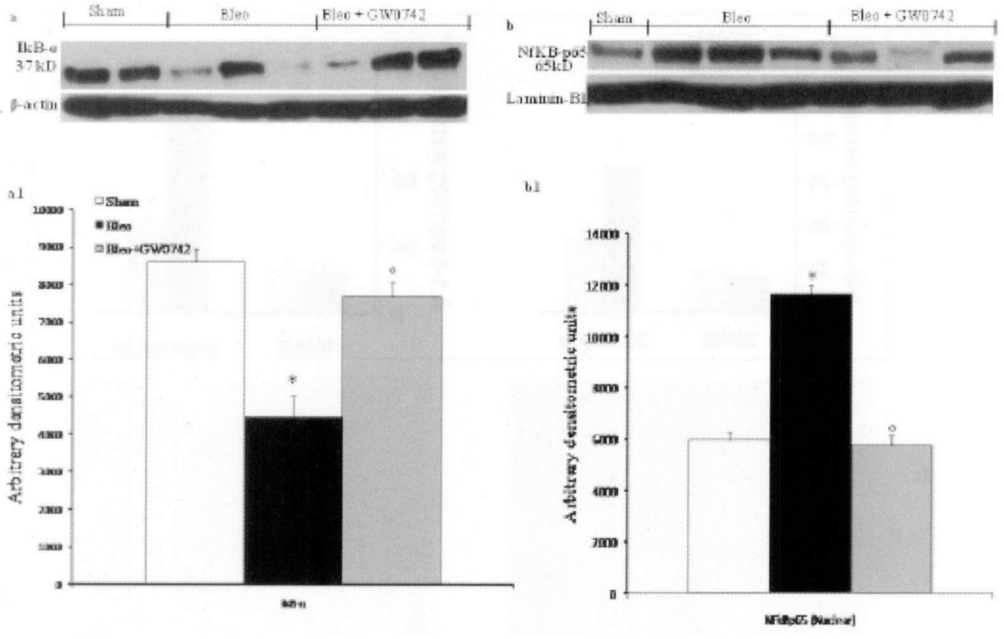

Fig. 4. *Western blot analysis detected a basal level of IkB-α (a, densitometry analysis a1) in the lung tissues of sham-operated animals, whereas in instilled mice, IkB-α levels were substantially reduced (a, densitometry analysis a1). GW0742 prevented bleomycin-induced IkB-α degradation, with IkB-α levels observed in these animals similar to those of the sham-operated mice (a, densitometry analysis a1). In addition, bleomycin caused a significant increase of NF-kB p65 levels in the nuclear fractions from lung tissues, compared to the sham-operated mice (b, densitometry analysis b1). GW0742 treatment significantly reduced the levels of NF-kB p65 in the lung (b, densitometry analysis b1). The results in a1 and b1 are expressed as mean ± s.e.mean from three blots. Data are expressed as arbitrary densitometry units and are mean ± standard deviation from n=10 mice for each group. *P<0.01 vs sham-operated mice, °P<0.01 vs bleomycin + vehicle.*

compared with sham-operated mice (Fig.5Aa, see densitometry analysis Aa1). In contrast, a significant decrease in iNOS expression was clearly observed in the BLEO-instillated mice treated with GW0742 (Fig. 5Aa, see densitometry analysis Aa1).

Moreover, immunohistochemical localization for iNOS showed no positive staining in the lung tissues obtained from sham animals (data not shown). On the contrary, lung sections obtained from BLEO-instilled mice revealed positive staining for iNOS (Fig. 5Ab, see densitometry analysis Ad), while no staining for iNOS was found in the lungs of BLEO-instilled mice that had been treated with GW0742 (Fig. 5Ac, see densitometry analysis Ad).

Immunohistochemical analysis of lung sections obtained from BLEO-instilled mice also revealed positive staining for nitrotyrosine (Fig. 5Ba, see densitometry analysis Be). In mice treated with GW0742, positive staining for nitrotyrosine was significantly reduced (Fig. 5Bc, see densitometry analysis Be). Moreover, immunohistochemical analysis of lung sections obtained from BLEO-instilled mice also revealed a positive staining for PAR (Fig. 5Bb, see densitometry analysis Be). In contrast, no staining for PAR was found in the lungs of BLEO-instilled mice treated with GW0742 (Fig. 5Bd, see densitometry analysis Be). There was no staining for either nitrotyrosine or PAR in lungs obtained from the sham group of rats (data not shown).

Effect of GW0742 on MAPK signal-transduction pathway

To investigate the cellular mechanisms by which GW0742 may attenuate the development of BLEO-induced inflammation, we evaluated the phosphorylation of ERK, causing activation of the MAPK pathways. In sample of lung, Western blot showed that BLEO caused a significant increase of phosphorylated ERK (p-ERK, Fig. 6a, see densitometry analysis a1), while GW0742

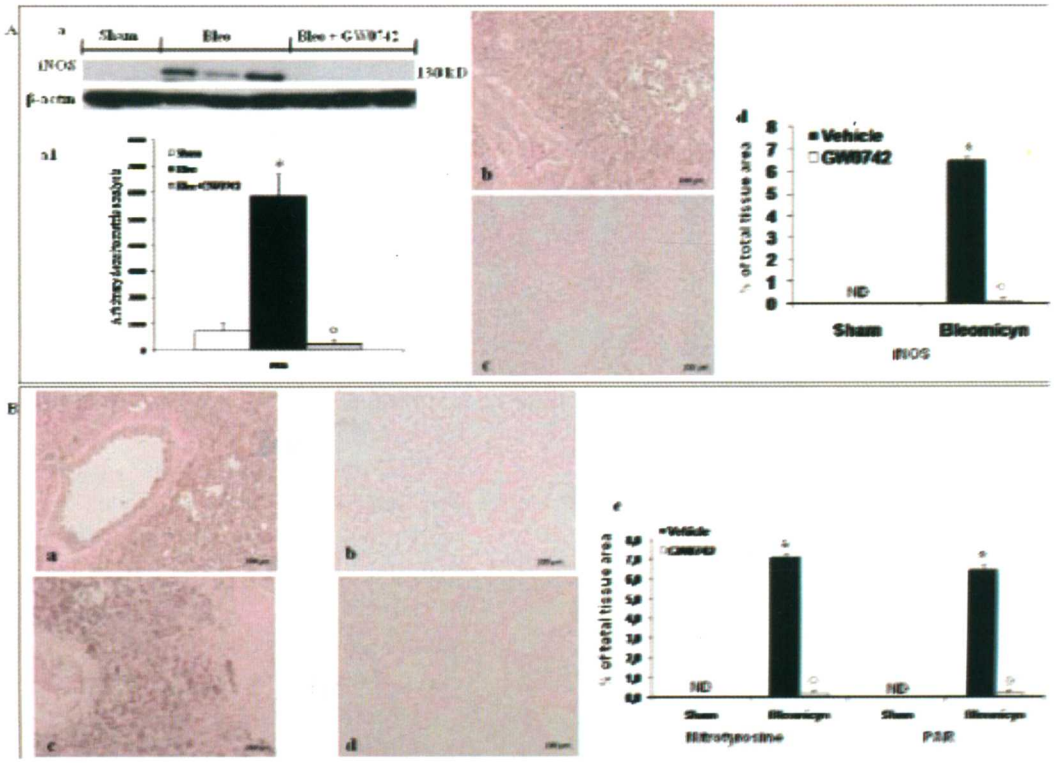

Fig. 5. *iNOS expression was assessed in samples of pulmonary tissue by Western blot analysis (Aa, densitometry analysis Aa1). A significant increase in iNOS expression was demonstrated in samples of lung obtained from BLEO-instilled mice, when compared with sham-operated mice (Aa, densitometry analysis Aa1). In contrast, a significant decrease in iNOS expression was clearly observed in BLEO-instilled mice treated with GW0742 (Aa, see densitometry analysis Aa1). The results in a1 are expressed as mean ± s.e.mean from three blots. Data are expressed as arbitrary densitometry units and are mean ± standard deviation from n=10 mice for each group. *P<0.01 vs sham, °P<0.01 vs bleomycin + vehicle. Moreover, immunohistochemical localization for iNOS showed that lung sections obtained from BLEO-instilled mice revealed positive staining for iNOS (Ab), while no staining for iNOS was found in the lungs of BLEO-instilled mice that had been treated with GW0742 (Ac). Immunohistochemical analysis of lung sections obtained from mice treated with BLEO also revealed positive staining for nitrotyrosine (Ba), while GW0742-treatment significantly reduced positive staining for nitrotyrosine (Bc). Moreover, immunohistochemical analysis of lung sections obtained from BLEO-instilled mice also revealed a positive staining for PAR (Bb). In contrast, no staining for PAR was found in the lungs of GW0742-treated mice (Bd).Densitometry analysis (Ad and Be) of immunohistochemistry photographs (n=5 photos from each sample collected from all mice in each experimental group) for iNOS (Ad), nitrotyrosine and PAR (Be) was assessed. The assay was carried out by using AxioVision on a personal computer. The figure is representative of at least three experiments performed on different experimental days. Data are expressed as % of total tissue area and are mean ± standard deviation from n=10 mice for each group. *P<0.01 vs sham, °P<0.01 vs bleomycin + vehicle.*

treatment resulted in a significant decrease of p-ERK expression (Fig. 6a, see densitometry analysis a1). No significant changes were observed in the ERK-2 expression (Fig. 6a).

Effects of GW0742 on apoptosis in lung tissues after BLEO-induced lung injury

To investigate whether acute lung inflammation was associated with cell death by apoptosis we measured TUNEL-like staining in lung tissues. Seven days after BLEO instillation, lung tissues demonstrated a marked appearance of dark brown apoptotic cells and intercellular apoptotic fragments (Fig. 7Aa, see cell count Ac). In contrast, no apoptotic cells or fragments were observed in tissues obtained from GW0742-treated mice (Fig. 7Ab, see

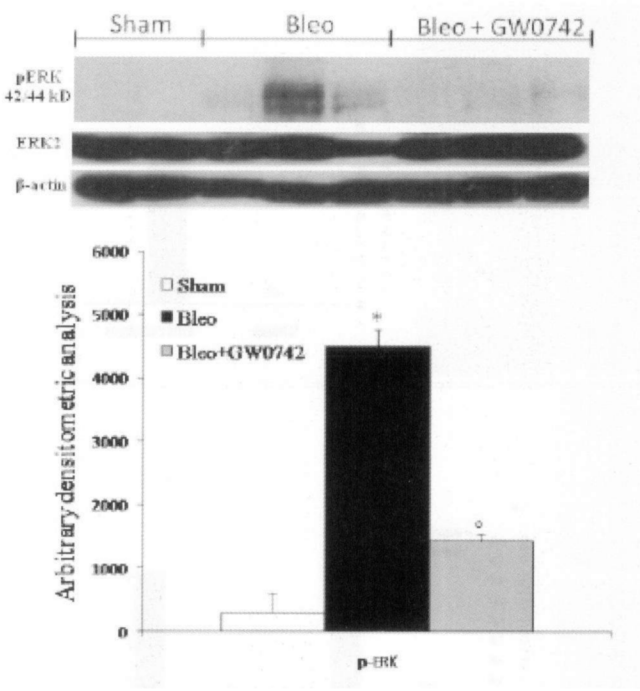

Fig. 6. *In sample of lung, Western blot showed that BLEO-administration caused a significant increase of phosphorylated ERK, p-ERK (6a, densitometry analysis a1), while GW0742 treatment resulted in a significant decrease of p-ERK expression (6a, densitometry analysis a1). No significant changes were observed in the ERK-2 expression (6a). The results in a1 are expressed as mean ± s.e.mean from three blots. Data are expressed as arbitrary densitometry units and are mean ± standard deviation from n=10 mice for each group. *P<0.01 vs sham-operated mice, °P<0.01 vs bleomycin + vehicle.*

cell count Ac). Similarly, no apoptotic cells were observed in the lungs of sham-operated mice (data not shown).

Effects of GW0742 on Fas-ligand expression after BLEO-instillation

Immunohistological staining for Fas ligand in the lung tissue was also determined 7 days after BLEO-instillation. Lung sections from sham-operated mice did not stain for Fas ligand (data not shown), whereas pulmonary sections obtained from instilled mice exhibited positive staining for Fas ligand (Fig. 7Ba, see densitometry analysis Bc). GW0742 reduced the degree of positive staining for Fas ligand in the lung tissues (Fig. 7Bb, see densitometry analysis Bc).

Western blot analysis and Immunohistochemistry for Bax and Bcl-2 after BLEO instillation

The presence of Bax and Bcl-2 in lung homogenates was investigated by Western blot 7 days after BLEO instillation. A basal level of Bax was detected in lung tissues obtained from sham-treated animals (Fig. 8a, see densitometry analysis a1). Bax levels were substantially increased in the lung tissues from instilled mice (Fig. 8a, see densitometry analysis a1). In contrast, GW0742 treatment prevented the bleomycin-induced Bax expression (Fig. 8a, see densitometry analysis a1).

A basal level of Bcl-2 was detected in lung tissues obtained from sham-treated animals (Fig. 8b, see densitometry analysis b1). Bcl-2 levels were substantially reduced in the lung tissues from instilled mice (Fig. 8b, see densitometry analysis b1). In contrast, GW0742 treatment significantly attenuated the bleomycin-induced reduction of Bcl-2 expression (Fig. 8b, see densitometry analysis b1).

Moreover, lung samples were also collected 7 days after BLEO-instillation for immunohistological staining for Bax and Bcl-2. Lung sections taken from sham-operated mice did not stain for Bax (data not shown), whereas the tissue obtained from instilled mice exhibited positive staining for Bax (Fig. 8d). GW0742 treatment reduced the degree of positive staining for Bax in mice subjected to BLEO-induced lung injury (Fig. 8f, see densitometry analysis h).

Lung tissue extracted from sham-operated mice demonstrated positive staining for Bcl-2 (Fig. 8c, see densitometry analysis h), while in instilled mice staining for Bcl-2 was absent (Fig. 8e, see densitometry analysis h). GW0742-treatment significantly attenuated the loss of positive staining for Bcl-2 in the lung of mice subjected to BLEO-induced injury (Fig. 8g, see densitometry analysis h).

DISCUSSION

It is well known that intratracheal administration of bleomycin results in direct damage initially to alveolar epithelial cells and following development of neutrophilic and lymphocytic pan-alveolitis (11). We showed that the treatment of mice with the PPARβ/δ agonist attenuates the migration of polymorphonuclear cells. Moreover, a consequence of the immediate response to the bleomycin-injury is

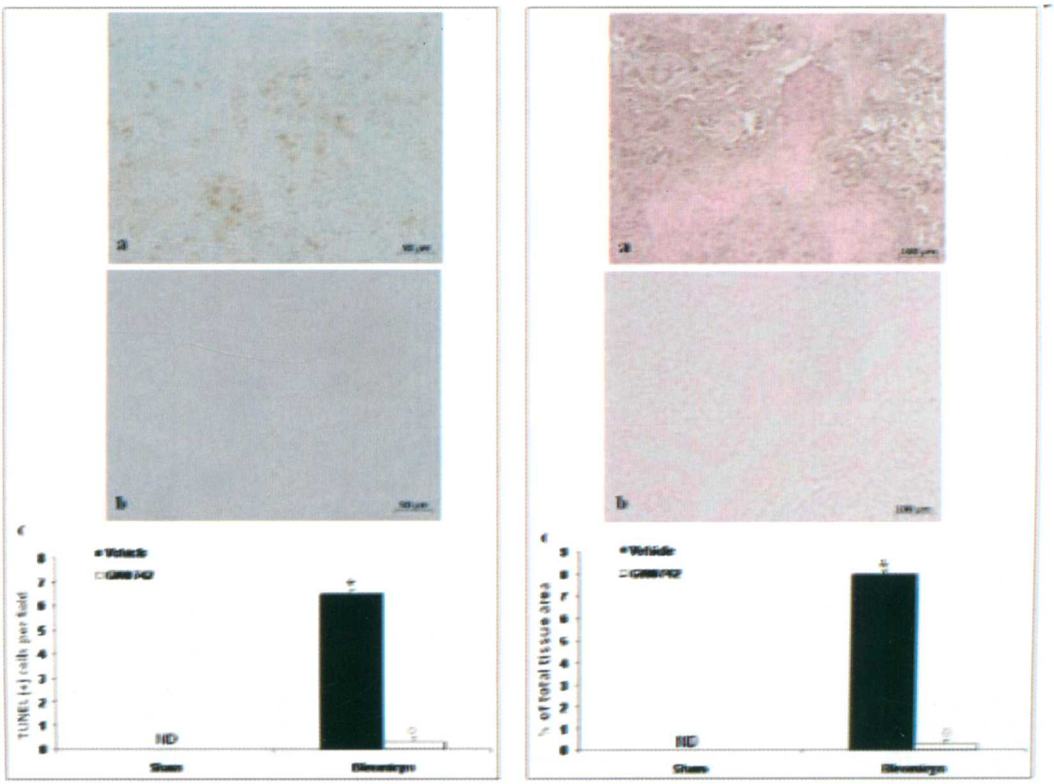

Fig. 7. *TUNEL-like staining in lung tissues showed that 7 days after BLEO administration, lung tissues demonstrated a marked appearance of dark brown apoptotic cells and intercellular apoptotic fragments (Aa, cell count Ac). In contrast, no apoptotic cells or fragments were observed in tissues obtained from BLEO-mice treated with GW0742 (Ab, cell count Ac). Moreover, immunohistological staining for Fas ligand in the lung tissue was also determined 7 days after BLEO administration. Pulmonary sections obtained from bleomycin-instilled mice exhibited positive staining for Fas ligand (Ba, densitometry analysis Bc). GW0742 reduced the degree of positive staining for Fas ligand in the lung tissues (Fig. 7Bb, densitometry analysis Bc). The number of TUNEL positive (Ac) cells/high-power field was counted in 5 to 10 fields for each coded slide. Densitometry analysis (Bc) of immunohistochemistry photographs (n=5 photos from each sample collected from all mice in each experimental group) for Fas Ligand was assessed. The assay was carried out by using AxioVision on a personal computer. The figure is representative of at least three experiments performed on different experimental days. Data are expressed as % of total tissue area and are mean ± standard deviation from n=10 mice for each group. *P<0.01 vs sham-operated mice, °P<0.01 vs bleomycin + vehicle.*

the production of cytokines, among which not only the TNF-α but also the IL-1β have a pivotal role, both produced by activated macrophages. TNF-α and IL-1β are involved in the pathogenesis of experimental lung injury.

This study clearly shows that PPAR β/δ activation plays an important role in decreasing the cytokine release due to bleomycin-instillation. Moreover, IL-1β mediates destruction of matrix collagens in diverse inflammatory diseases (including arthritis, periodontitis and pulmonary fibrosis, activating fibroblasts, cells that interact with matrix proteins through integrin-based adhesions), and induces activation of ERK and recruitment of phospho-ERK to focal complexes/adhesions (12). We proved that GW0742-treatment reduces the MAP kinase signalling pathway activation and the following damage to the lung triggered by ERK cascade, that have a central role in the activation of cellular processes such as proliferation, differentiation and

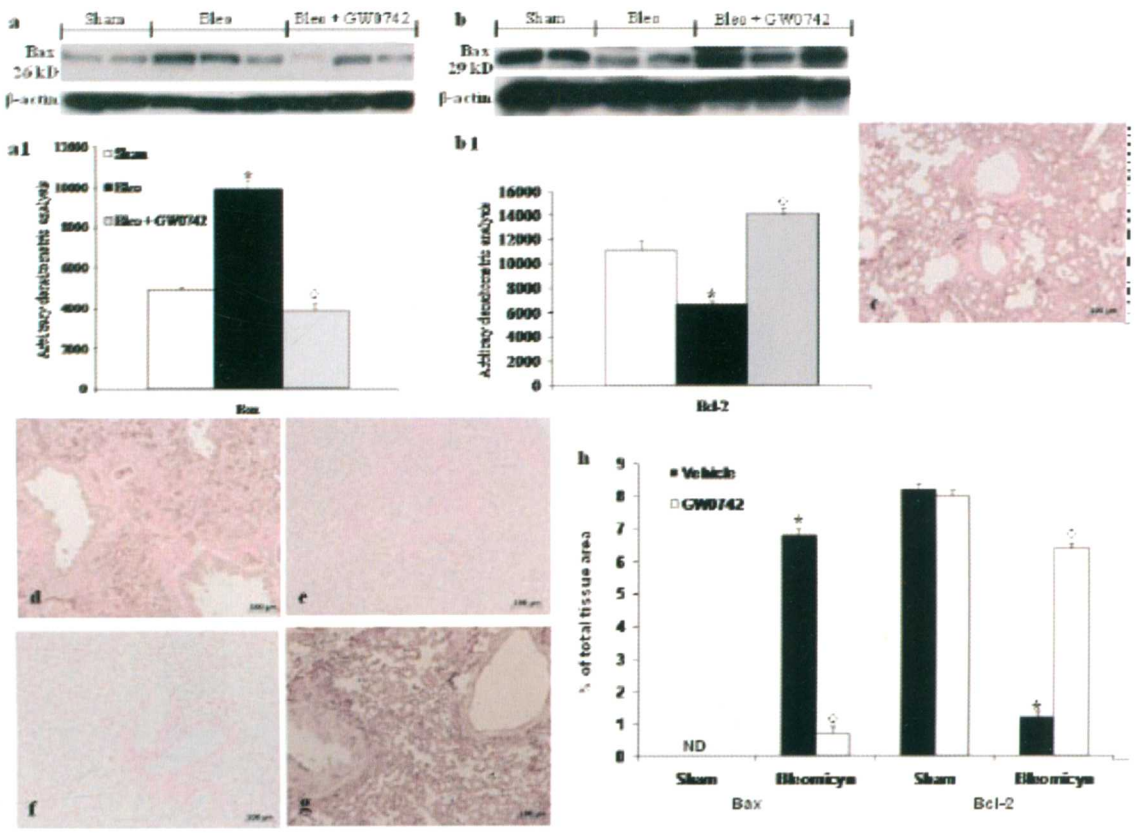

Fig. 8. *Western blot analysis, 7days after bleomycin administration showed a basal level of Bax in lung tissues obtained from sham-operated animals (a, densitometry analysis a1). Bax levels were substantially increased in the lung tissues from bleomycin-administered mice (a, densitometry analysis a1). In contrast, GW0742 treatment prevented the bleomycin-induced Bax expression (a, densitometry analysis a1). A basal level of Bcl-2 was detected in lung tissues obtained from sham-operated animals (b, densitometry analysis b1). Bcl-2 levels were substantially reduced in the lung tissues from bleomycin-administered mice (b, densitometry analysis b1). In contrast, GW0742 treatment significantly attenuated the bleomycin-induced reduction of Bcl-2 expression (b, densitometry analysis b1). The results in a1 and b1 are expressed as mean ± s.e.mean from three blots. Data are expressed as arbitrary densitometry units and are mean ± standard deviation from n=10 mice for each group. *P<0.01 vs sham-operated mice, °P<0.01 vs bleomycin + vehicle. Moreover, lung samples were also collected 7 days after BLEO administration for immunohistological staining for Bax and Bcl-2. Lung sections obtained from BLEO-treated mice exhibited positive staining for Bax (d, densitometry analysis h). GW0742 treatment reduced the degree of positive staining for Bax in mice subjected to BLEO-induced lung injury (f, densitometry analysis h). Moreover, lung tissue extracted from sham-operated mice demonstrated positive staining for Bcl-2 (c, densitometry analysis h), while in BLEO-treated mice staining for Bcl-2 was absent (e, densitometry analysis h). GW0742-treatment significantly attenuated the loss of positive staining for Bcl-2 in the lung of mice subjected to BLEO-induced injury (g, densitometry analysis h). Densitometry analysis (h) of immunohistochemistry photographs (n=5 photos from each sample collected from all mice in each experimental group) for Bax and Bcl-2 was assessed. The assay was carried out by using AxioVision on a personal computer. The figure is representative of at least three experiments performed on different experimental days. Data are expressed as % of total tissue area and are mean ± standard deviation from n=10 mice for each group. *P<0.01 vs sham-operated mice, °P<0.01 vs bleomycin + vehicle.*

oncogenic transformation (13).

A number of studies in mice and in humans have shown that PPAR agonists exhibit anti-inflammatory effects mainly through the inhibition of transcription factors that positively regulate pro-inflammatory genes, including, among others, the Nuclear Factor-κB (14). PPAR β/δ activation prevents the activation of NF-κB so that GW0742-treatment blocks the

bleomycin-induced alteration between IkBα/NFkB, reporting their association to physiological levels.

Moreover, bleomycin is thought to induce lung injury through the production of oxidant species and for its ability to cause DNA strand breakage (15).

Indeed, exposure of tissues and cells to these pro-inflammatory cytokines also results in the expression of the inducible isoform of NOS (iNOS), which leads to the formation of nitric oxide and to the following oxidative stress.

In this study, we have the evidence that GW0742-treated mice develop a lower degree of cytotoxic effects due to NO formation, and, as consequence, also a reduction of the nitrosative stress, measured by tissue localization of nitrotyrosine, a reactive oxidant formed by the rapid reaction of NO with superoxide anions and marker of peroxynitrite formation (16).

Moreover, we showed that the role of PPARβ/δ is also associated to a decrease in the activation of the nuclear enzyme poly (ADP-ribose) synthetase (PARS) which causes depletion of intracellular NAD and ATP pools and ultimately cell death ("PARS suicide hypothesis") (17), as consequence of the DNA single strand breaks due to peroxynitrite formation (18).

Other consequences of these events are the activation of FAS receptor and of the apoptosis pathway, mediated by a decrease of anti-apoptotic members (Bcl-2, Bcl-xL), allowing Bax to translocate to the outer mitochondrial membrane, thus permeabilizing it and facilitating release of pro-apoptotic proteins (19). Our data show that the bleomycin-induced FAS ligand expression with the consequent alteration of Bax/Bcl-2 balance, is reduced by the treatment with GW0742, confirming that GW0742-treatment can modulate the apoptosis pathways that otherwise lead to presence of large areas of pulmonary disruption.

In conclusion, this study provides the evidence that GW0742, a selective ligand of Peroxisome Proliferator-Activated Receptors β/δ, has a potential therapeutic role in the treatment of lung inflammation.

ACKNOWLEDGEMENTS

This work was supported by a grant from IRCCS Centro Neurolesi "Bonino-Pulejo". We thank Tiziana Genovese and Carmelo La Spada for their excellent technical assistance during this study, Mrs Caterina Cutrona for secretarial assistance and Miss Valentina Malvagni for editorial assistance with the manuscript.

REFERENCES

1. Green FH. Overview of pulmonary fibrosis. Chest 2002; 122(S):334-9.
2. Selman M, King TE, Pardo A. Idiopathic pulmonary fibrosis: prevailing and evolving hypotheses about its pathogenesis and implications for therapy. Ann Intern Med 2001; 134:136-51.
3. Sleijfer S. Bleomycin-induced pneumonitis. Chest 2001; 120:617-24.
4. Moore BB, Hogaboam CM. Murine models of pulmonary fibrosis. Am J Physiol 2008; 294:152-60.
5. Piqueras L, Sanz MJ, Perretti M, et al. Activation of PPAR β/δ inhibits leukocyte recruitment, cell adhesion molecule expression, and chemokine release. J Leukoc Biol 2009; 86:115-22.
6. Staels B. PPAR agonists and the metabolic syndrome. Therapie 2007; 62:319-26.
7. Chintalgattu V, Harris GS, Akula SM, et al. PPAR-gamma agonists induce the expression of VEGF and its receptors in cultured cardiac myofibroblasts. Cardiovasc Res 2007; 74:140-50.
8. Piqueras L, Reynolds AR, Hodivala-Dilke KM, et al. Activation of PPARbeta/delta induces endothelial cell proliferation and angiogenesis. Arterioscler Thromb Vasc Biol 2007; 27:63-9.
9. Clark RB. The role of PPARs in inflammation and immunity. J Leukoc Biol 2002; 71:388-400.
10. Bishop-Bailey D. Peroxisome proliferator-activated receptor beta/delta goes vascular. Circ Res 2008; 102:146-7.
11. Janick-Buckner D, Ranges GE, Hacker MP. Alteration of bronchoalveolar lavage cell populations following bleomycin treatment in mice. Toxicol Appl Pharmacol 1989; 100:465-73.
12. Herrera Abreu MT, Wang Q, Vachon E, et al. Tyrosine phosphatase SHP-2 regulates IL-1 signalling in fibroblasts through focal adhesions. J Cell Physiol 2006; 207:132-43.
13. Chuderland D, Seger R. Protein-protein interactions in the regulation of the extracellular signal-regulated kinase. Mol Biotechnol 2005; 29:57-74.
14. Lucas R, Verin AD, Black SM, et al. Regulators

of endothelial and epithelial barrier integrity and function in acute lung injury. Biochem Pharmacol 2009; 77:1763-72.

15. Lown JW, Sim SK. The mechanism of the bleomycin-induced cleavage of DNA. Biochem Biophys Res Commun 1977; 77:1150-7.
16. Pryor WA, Squadrito GL. The chemistry of peroxynitrite: a product from the reaction of nitric oxide with superoxide. Am J Physiol 1995; 268:699-722.
17. Zingarelli B, O'Connor M, Wong H, et al. Peroxynitrite-mediated DNA strand breakage activates poly-adenosine diphosphate ribosyl synthetase and causes cellular energy depletion in macrophages stimulated with bacterial lipopolysaccharide. J Immunol 1996; 156:350-8.
18. Inoue S, Kawanishi S. Oxidative DNA damage induced by simultaneous generation of nitric oxide and superoxide. FEBS letters 1995; 371:86-8.
19. Wajant H. The Fas signalling pathway: more than a paradigm. Science 2002; 296:1635-6.